Metal Substitution and the Active Site of Carbonic Anhydrase

D. R. Garmer[†] and M. Krauss*[,‡]

Contribution from the Department of Physiology and Biophysics, Mt. Sinai Medical Center, New York, New York 10029, and Center for Advanced Research in Biotechnology, National Institute of Standards and Technology, Gaithersberg, Maryland 20899.
Received November 8, 1991

Abstract: A cluster model is used to analyze the variation with metal substitution of both the coordination number at the active site of carbonic anhydrase and the proton affinity of OH^- bound to the metal cation. Experimentally the native zinc and cobalt enzymes are comparably active with respect to the hydration of carbon dioxide, but the cadmium and manganese enzymes are essentially inactive. A significant difference in the cluster behavior between the zinc and cobalt models and those for manganese and cadmium is found for the coordination number of the active high pH form. Energetics of water binding indicates the first-shell coordination number in the high-pH active form expands to five for cadmium and manganese from four in the native zinc or cobalt enzymes. The stronger binding of water in the first shell would make the approach of the carbon dioxide substrate more difficult or otherwise disrupt the binding to the first shell. We suggest that this postulated inhibitory effect of a strongly bound water ligand accounts for the lower activity of cadmium and manganese carbonic anhydrase. On the other hand, there is nothing in the electronic structure of the cadmium and manganese high-pH complexes that would indicate a reduction in the nucleophilicity of the bound OH^- relative to that for zinc and cobalt. The calculated proton affinities in four- and five-coordinate models agree with the relative behavior of the experimental pK_a of the active nucleophile in carbonic anhydrase. Adding the fifth water ligand in either the first or second shell increases the absolute energy differences in the proton affinities but retains the correct order. This result implies that all metal-substituted carbonic anhydrases would be active but shifted in pH range except for the change in the coordination number. Although the electrostatic effect of the metal cation is dominant in lowering the proton affinity, there are substantial differential reaction field solvation and correlation contributions. Continuum effects are estimated relative to the first shell complex. Hydration enthalpies are calculated for the metal–aquo complexes to test the model for first-shell complexes. Considering the Jahn–Teller distortion and large correlation effects for the electronically degenerate cobalt complex, the relative values of the hydration enthalpies of the hexa–aquo complexes of zinc, cobalt, and manganese are in agreement with experiment, but cadmium is sufficiently different to suggest that the hydration coordination number may be larger than six. The order of the calculated binding energies relative to the hydration enthalpies with metal substitution qualitatively agrees with the order of experimental stability constants. The native zinc is the most stable with cadmium closest for both the low and high pH model clusters. Both cobalt and manganese are substantially less bound.

1. Introduction

Metal substitution for the native zinc in carbonic anhydrase (ZnCA) probes the electronic and geometric structure of the active site and thus provides insight into the mechanism of action. Carbonic anhydrase catalyzes the reversible hydration of carbon dioxide. It is widely accepted that the nucleophile is OH^- bound to the metal. The field of the metal cation bound to a tripod of histidine residues reduces the effective proton affinity of M–OH so that it is available to hydrate carbon dioxide above pH 7.[1,2] The simplest view of the effect of metal substitution is that the concentration of active enzyme at a given pH is determined by the stability of metal binding and the shift in the effective proton affinity of the active metal bound hydroxide form of the enzyme. However, this does not explain the near absence of activity of the cadmium and manganese enzymes[3] even in the pH range appropriate for a high concentration of OH^- bound to the metal. Cobalt is the only metal with a comparable activity with respect to hydration of carbon dioxide[3] as the native zinc. Small variations in the nucleophilicity of the OH^- induced by metal cation substitution are presumably unimportant because the hydrolysis step is not rate-limiting. Proton transfer from the reactive center to a histidine separated by a hydrogen-bonded network of water and/or protein residues is rate-limiting for the zinc enzyme.[2,4,5] However, there is the possibility that the mechanism is altered by the metal substitution. The catalytic behavior also requires the maintenance of an active site stereochemistry upon metal substitution[6] as well as the presence of the OH^- nucleophile. In this study we search for a dramatic difference in behavior manifest in the structure of the first-shell metal complex which could alter either the rate or the rate-limiting step upon metal substitution.

In two previous studies we have analyzed the mechanism of native CA[7] and the relation between the structure and the spectra of the active site for cobalt(II) substituted CA[8] using ab initio cluster methods. These studies have shown that first-shell cluster calculations of the ligand binding energies and the effective proton affinity represent the dominant metal interaction and allow comparative studies of ligand binding, stereochemistry, and reactivity. In a recent work, a cluster model with appropriate thermodynamic and solvent continuum corrections provided insight into the relation between the structure of the two metal binding sites in the protease Subtilisin bpn' and competitive binding among calcium, magnesium, and sodium cations.[9] A similar cluster model is applied in the present work to analyze the effect of the substitution of cobalt, cadmium, and manganese cations for zinc on the electronic structure and stereochemistry of the active, hydroxyl-containing, first-shell complexes as well as the effective pK_a of metal-bound hydroxide.

Cobalt, cadmium, and manganese bind to the CA active site normally occupied by a zinc dication in the active enzyme.[6] The visible spectra of $Co^{II}CA$ has been interpreted to support a four-coordinate stereochemistry analogous to zinc.[10] Since the protein environment around the active site is not considered at present, no distinction is made of the different isozymes where differences in environmental fields or hydrogen bonding patterns have substantial effects on enzyme activity and pK_a[2] but still leave physiologically active enzymes as opposed to substitution of

[†] Mt. Sinai Medical Center.
[‡] Center for Advanced Research in Biotechnology.

(1) Pullman, A. *Ann. N.Y. Acad. Sci.* **1981**, *367*, 340.
(2) Silverman, D. N.; Lindskog, S. *Acc. Chem. Res.* **1988**, *21*, 30.
(3) Lindskog, S. *Adv. Inorg. Chem.* **1982**, *4*, 115.
(4) Eriksson, E. A.; Jones, T. A.; Liljas, A. In *Zinc Enzymes*; Bertini, I., Luchinat, C., Maret, W., Zeppezauer, M., Eds.; Birkhauser: Boston, 1986; pp 317-328.
(5) Eriksson, E. A.; Jones, T. A.; Liljas, A. *Proteins* **1988**, *4*, 273.
(6) Bertini, I.; Luchinat, C.; Scozzafava, A. *Structure Bonding* **1982**, *48*, 46.
(7) Kraus, M.; Garmer, D. R. *J. Am. Chem. Soc.* **1991**, *113*, 6426.
(8) Garmer, D. R.; Krauss, M. *Int. J. Quantum Chem.* **1992**, *42*, 1469.
(9) Krauss, M.; Stevens, W. J. *J. Am. Chem. Soc.* **1990**, *112*, 1460.
(10) Bertini, I.; Luchinat, C. *Acc. Chem. Res.* **1983**, *16*, 272.

0002-7863/92/1514-6487$03.00/0

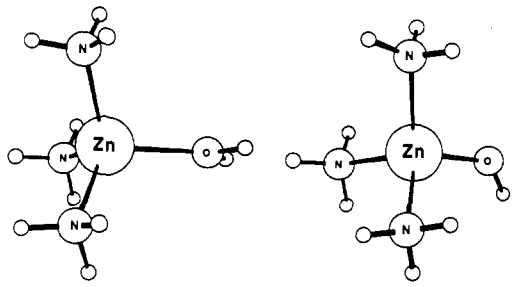

Figure 1. Schematic structures of four-coordinate models: (a) $Zn(NH_3)_3OH_2$ and (b) $Zn(NH_3)_3OH^-$.

cadmium and manganese. It has been noted that the coordination behavior of the metal center at high pH is probably similar in all three isozymes since the visible spectra of the cobalt-substituted isozymes are similar.[11] Binding to the apoenzyme and perturbed angular correlation of X-rays in CdCA has been interpreted for tetrahedral coordination of the cadmium cation with ionization of the metal-bound water ligand at a pK of about 9.[12] The theoretical model incorrectly assumed the bonding of Cd^{2+} to the first-shell ligands to be predominantly covalent so the first-shell structure requires examination. The NMR of the cadmium nucleus has also supported the metal role to lower the deprotonation energy of metal-bound water.[13] Manganese is known to bind at the active site but here is little direct evidence of the stereochemistry.[6,14] MnCA is found to be much less stable than the native enzyme with the ZnCA dissociation rate about five orders of magnitude smaller.[15] The stability constants of the metalloenzymes are summarized in a review by Lindskog.[3]

The pK_a of CoCA is slightly smaller than that of ZnCA.[3] On the other hand, the pK_a's of MnCA and CdCA are about 1 and 2 units, respectively, larger than that of ZnCA.[3] Since the active sites of ZnCA, CdCA, and CoCA are reported to be experimentally comparable, the relative energetics of water and hydroxyl anion binding to the metal could be obtained from first-shell cluster calculations to determine the relative pK_a as a test of the cluster model. We shall assume an analogous model for MnCA and determine the consequences.

Both four- and five-coordinate models are considered. At high pH zinc and cobalt clusters energetically favor four-coordination.[9] For low pH a five-coordinate structure is favored if all ligands are neutral, but deprotonation of the His-119 is predicted[9] and will substantially reduce the binding energy for the second water. Experimentally both four- and five-coordinate structures are suggested.[10,16] The effects of protein fields are assumed to be similar for the different metal complexes, and energy stabilization of the clusters is estimated from the charge and multipole moments of the clusters with a continuum model. The calculated cluster binding energies when compared to the hydration enthalpies of these divalent cations are used to rank the relative stabilities of the substituted enzymes. The calculation of the hydration enthalpies of the divalent cations provides another guage for judging the protein cluster model.

2. Method

The initial model system is a metal complex of three ammonias and a water or hydroxyl ligand bound to the metal dication (see Figure 1). Ammonia ligands are substituted for imidazole or histidyl ligands that form a tripod for the metal dication in CA. The complex with the water ligand represents the low-pH active site and with hydroxyl the high-pH form. Approximate cluster models have been used to model the active site of carbonic anhydrase[1,7,8] and, in a recent calculation, to model the behavior of the pK_a of zinc-bound water.[17] A test of the suitability of the substitution of ammonia for imidazole that shows the overall charge description of the metal complex is unaffected will be described below. The metal, oxygen, and nitrogen atom cores are represented by compact effective core potentials derived by Stevens et al.[18,19] All the metal basis sets include a total of four sp functions for both the valence and penultimate shells. The metal d basis contains two independent functions using a (41) contraction[20] rather than the (411) contraction given in ref 19. The s and p basis is roughly double-ζ (CEP-31G) for all atoms, but a single d polarization function with a $\zeta = 0.85$ was added for oxygen.

The geometries are energy gradient optimized at the unrestricted Hartree–Fock (UHF) level with this basis using either the GAMESS[21] or GAUSSIAN[22] system of codes. Geometrical characteristics of the four-coordinate clusters are given in Table I. All are tetrahedral to within about 5° for the angles between the ligands and so are compatible with the observed structure of the histidine tripod at the CA active site. Binding energies (BE/UHF) given in Table II are obtained at these optimized geometries after adding a second, diffuse d polarization shell ($\zeta = 0.2$) to the oxygen atoms. The larger diffuse basis is found to improve the monomer moments and polarizabilities ensuring a more

Table I. Characteristics of CA and Hydration Models

cluster	R(MO), Å	R(MN), Å	a(MOH), deg	Born radius, Å
$ZnOH(NH_3)_3$	1.83	2.13	131	3.57
$CoOH(NH_3)_3$	1.86	2.17	136	3.61
$MnOH(NH_3)_3$	1.89	2.29	165	3.71
$CdOH(NH_3)_3$	2.05	2.38	129	3.81
$ZnOH_2(NH_3)_3$	2.09	2.08		3.58
$CoOH_2(NH_3)_3$	2.12	2.13		3.63
$MnOH_2(NH_3)_3$	2.21	2.25		3.74
$CdOH_2(NH_3)_3$	2.34	2.32		3.83
$Zn(OH_2)_6$	2.14			3.64
$Co(OH_2)_6$	2.16			3.66
$Mn(OH_2)_6$	2.26			3.76
$Cd(OH_2)_6$	2.37			3.87
$Cd(OH_2)_8$	2.48			3.98

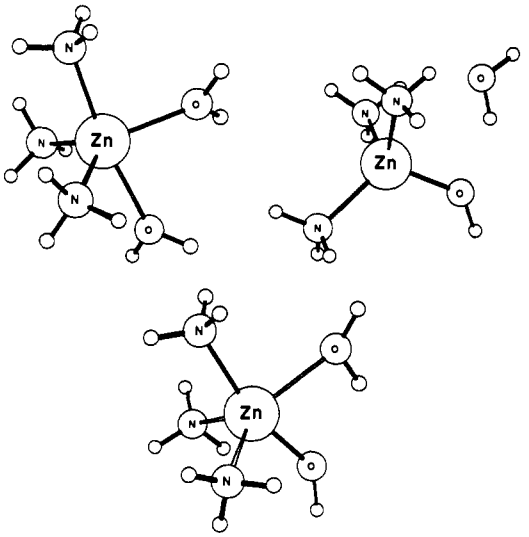

Figure 2. Schematic structures for models with added water: (a) $Zn(NH_3)_3(OH_2)_2$, (b) $Zn(NH_3)_3OH^-\cdots OH_2$, and (c) $Zn(NH_3)_3(OH^-)(OH_2)$.

(11) Lindskog, S. In *Zinc Enzymes*; Bertini, I., Luchinat, C., Maret, W., Zeppezauer, M., Eds.; Birkhauser: Boston, 1986; pp 307–316.
(12) Bauer, R.; Limkilde, P.; Johansen, J. T. *Biochemistry* **1976**, *15*, 334.
(13) Armitage, M.; Uiterkamp, A. J. M. S.; Chlebowski, J. F.; Coleman, J. E. *J. Magn. Reson.* **1978**, *29*, 375.
(14) Lanir, A.; Navon, G. *Biochemistry* **1972**, *11*, 3536.
(15) Wilkins, R. G.; Williams, K. R. *J. Am. Chem. Soc.* **1974**, *96*, 2242.
(16) Satish, K. N.; Christianson, D. W. *J. Am. Chem. Soc.* **1991**, *113*, 9455.
(17) Bertini, I.; Luchinat, C.; Rosi, M.; Sgamellotti, A.; Tarantelli, F. *Inorg. Chem.* **1990**, *29*, 1460.
(18) Stevens, W. J.; Basch, H.; Krauss, M. *J. Chem. Phys.* **1984**, *81*, 6026.
(19) Stevens, W. J.; Basch, H.; Jasien, P. G.; Krauss, M. Relativistic Compact Effective Potentials and Efficient, Shared-Exponent Basis Sets for the Third-, Fourth-, and Fifth-Row Atoms. *Can. J. Chem.* accepted for publication.
(20) Rappe, A. K.; Smedley, T. A.; Goddard, W. A. *J. Phys. Chem.* **1981**, *85*, 2607.
(21) Schmidt, M. W.; Boatz, J. A.; Baldridge, K. K.; Koseki, S.; Gordon, M. S.; Elbert, S. T.; Lam, B. GAMESS *QCPE Bull.* **1987**, *7*, 115.
(22) Frisch, M. J.; Head-Gordon, M.; Trucks, G. W.; Foresman, J. B.; Schlegel, H. B.; Raghavachari, K.; Robb, M. A.; Binkley, J. S.; Gonzalez, C.; Defrees, D. J.; Fox, D. J.; Whiteside, R. A.; Seeger, R.; Melius, C. F.; Baker, J.; Martin, R. L.; Kahn, L. R.; Stewart, J. J. P.; Topiol, S.; Pople, J. GAUSSIAN 90, Gaussian, Inc., Pittsburgh, 1990.

Table II. Energetics (kJ/mol) of Tetrahedral CA Models

cluster	BE(UHF)	disp	dBE(MP2)	ZPE	*E*(Born)	proton affinity	rel ΔH
$ZnOH(NH_3)_3$	2394	0.4	38.9	−53.1	189.9	1121	0
$CoOH(NH_3)_3$	2321	0.8	71.5	−54.4	186.2	1114	50.7
$MnOH(NH_3)_3$	2153	3.3	41.8	−49.8	179.9	1125	63.2
$CdOH(NH_3)_3$	2079	1.7	49.0	−49.0	184.1	1137	27.2
$ZnOH_2(NH_3)_3$	1351	2.5	44.4	−51.0	605.8		0
$CoOH_2(NH_3)_3$	1279	2.5	71.1	−52.3	599.1		55.7
$MnOH_2(NH_3)_3$	1126	2.5	48.1	−48.1	585.3		59.0
$CdOH_2(NH_3)_3$	1088	2.5	47.7	−46.4	570.7		11.3

Table III. Energetics (kJ/mol) for Adding a Water Molecule to the Four-Coordinate CA Model

cluster	water BE(UHF)	water ΔBE(MP2)	total water BE	*E*(Born)	proton[a,b] affinity	rel[a] ΔH/bind
$ZnOH(NH_3)_3\cdots OH_2$	72.8	19.2	92.0		1069[c]	0
$ZnOHOH_2(NH_3)_3$	24.3	2.9	27.2	175.7	1148	0
$Zn(OH_2)_2(NH_3)_3$	56.1	1.3	57.3	587.9		0
$MnOH(NH_3)_3\cdots OH_2$	73.6	19.2	92.9		1111[c]	62.3
$MnOHOH_2(NH_3)_3$	54.8	11.7	66.5	166.1	1151	23.4
$Mn(OH_2)_2(NH_3)_3$	89.5	10.9	100.4	563.2		20.1
$CdOHOH(NH_3)_3\cdots OH_2$	74.9	17.2	92.0		1112[c]	27.2
$CdOHOH_2(NH_3)_3$	46.4	3.3	49.8	173.6	1165	0.8
$Cd(OH_2)_2(NH_3)_3$	77.0	3.3	80.3	557.3		−16.3

[a] These quantities were obtained by adjusting the values from the corresponding complexes in Table II with the listed "total water BE". The disp, ΔBE(MP2), and ZPE corrections are effectively carried over which is justified by the small contribution they make to the differential comparison. [b] The proton affinities are calculated with the five-coordinate low-pH structural model for the protonated state. [c] Born energies of the tetrahedral models for the high-pH forms were used. This was done because the clusters are nonspherical and cannot be well approximated. The first shells strongly resemble those of the tetrahedral models and the H-bond strengths to the second shells are nearly identical.

Table IV. Energetics (kJ/mol) of Hydration Models

dication cluster	BE(UHF)	disp	ΔBE(MP2)	ZPE	*E*(Born)	free W	$-\Delta H$(hyd)
$Zn(OH_2)_6$	1364	41.0	19.7	−68.2	804.2	−159.0	2002 (2044)[a]
$Co(OH_2)_6$	1334	38.9	36.4	−66.5	809.6	−159.0	1994 (2054)[b]
$Mn(OH_2)_6$	1199	33.1	28.5	−66.5	787.4	−159.0	1823 (1845)
$Cd(OH_2)_6$	1118	27.2	28.9	−63.2	771.1	−159.0	1723 (1806)
$Cd(OH_2)_8$	1243	58.6	21.3	−97.1	711.3	−212.1	1725 (1806)
$Mn(OH_2)_8$	1305	67.4	20.1	−96.2	726.8	−212.1	1810
$Zn(OH_2)_4$	1139	13.8	28.0	−52.7	871.5	−105.9	1894
$Co(OH_2)_4$	1082	12.5	54.0	−49.8	861.5	−105.9	1854

[a] Experimental values from: Burgess, J. *Ions in Solution: Basic Principles of Chemical Interactions*; Elis Horwood Ltd.: London, England, 1988; p 55. [b] A small Jahn–Teller contribution to the ΔH(hyd) is discussed in the text.

accurate calculation of the dominant electrostatic component of ligand binding and protonation. A diffuse sp shell for proton affinity calculations of anions has usually been required. This additional basis shell is not required here because the hydroxyl strongly transfers charge to the dications and is not unusually diffuse. The CEP basis set sp shells also are more diffuse than the corresponding terms in commonly used all-electron DZ bases. The proton affinity is determined from the difference in water and hydroxyl cluster binding energies by using the proton affinity of hydroxyl anion (1739.7 kJ/mol). The relative binding energies are also determined with respect to the calculated difference in the hydration energies for the metal dications so these values can be related in Table II directly to the experimental stability constants.[3,15,23]

We have previously concluded that an additional water molecule can bind to the first shell for the low-pH complex.[7,8] Analogous models are constructed here and shown in Figure 2. Since the metal substitutioin could alter the coordination number, the water was added to the high-pH complex in both the first and second shells. The energetics of adding the water is summarized in Table III. Difficulties were encountered in optimizing UHF solutions with cobalt due to the presence of low-lying d virtual orbitals, but based on previous results for cobalt at fixed geometries we can assume that cobalt and zinc will have similar coordination numbers for the low- and high-pH complexes and behave similarly with respect to the effective proton affinity.

As a check on the relative accuracy of the important metal-to-oxygen distances and the local electronic structure and fields, the geometries of the hexaaquo species were also optimized and the hydration enthalpy estimated analogously to calculations done with the protein model complexes. The X-ray data for these hydrated dications are modeled for a six-coordinate first shell.[23] The ab initio structures are depicted in Figure 3a where the protons are seen to favor pointing at the oxygen atoms of

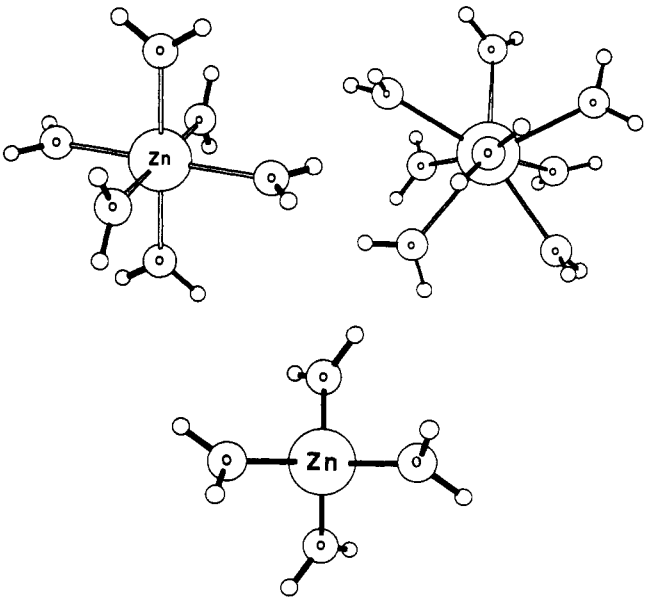

Figure 3. Schematic structures for the hydration model: (a) $M(OH_2)_6$, (b) $M(OH_2)_8$, and (c) $M(OH_2)_4$.

(23) Magini, M.; Licheri, G.; Paschina, G.; Piccaluga, G.; Pinna, G. *X-Ray Diffraction of Ions in Aqueous Solutions: Hydration and Complex Formation*; CRC Press, Inc.: Boca Raton, FL, 1988.

nearest-neighbor waters. However, cadmium is about the same size as calcium which may have a variable coordination number up to ten.[24] Therefore, we have examined larger complexes and found that a square antiprismatic complex with eight waters of S8 symmetry has metal-to-oxygen distances compatible with the X-ray values.[23] As seen in Figure 3b, the optimized geometry also has the protons oriented toward oxygen atoms on nearest-neighbor waters which stabilizes the complex. For completeness, the hydration energy for four-coordinate complexes (Figure 3c) was calculated for zinc and cobalt and found to be substantially smaller than the larger complexes. The energetics for the hydration complexes are given in Table IV.

The cobalt(II) complex in octahedral symmetry has a triply degenerate $^4T_1$ ground state. The optimized complex undergoes a Jahn–Teller distortion to a lower C_i symmetry. The distortion primarily involves the shortening of one opposed pair of Co–O contacts by 0.005 Å and an increase by 0.005 Å for another pair accompanied by a slight 2–3° rotation of each water molecule about its Co–O axis. This distortion from octahedral symmetry results in an energy lowering of 1.3 kJ/mol at the UHF level in the optimization basis. The energetic splitting of the $^4T_1$ term is much less than indicated by interpretation of the spectra of this complex,[25] but the geometric distortion is of similar magnitude to that deduced for the Co^{3+} hexammine excited states.[26]

A number of corrections are considered for the SCF binding energies. These are applied when computing the final proton affinities, relative binding enthalpies, and hydration enthalpies listed in Tables II–IV. Solvent corrections used the Born reaction field model for spherical cavities. The cavity surface was chosen to pass through the midpoint of idealized hydrogen bonds to a second-shell water since this worked well in a previous study of cation hydration.[9] It was found that this usually gave a radius of 1.5 Å larger than the radius of a best-fit sphere to the first-shell heavy-atom positions, so this was adopted as the standard method of defining a cavity. Induction energies from the cavity charge through the hexadecapole are summed as the Born energy listed in the tables. The hexadecapole is the lowest order non-zero moment for the hexaaquo species after the electronic charge and contributes less than one-tenth of the solvation energy for all the dication protein model complexes, suggesting that higher-order terms are unimportant. The hexadecapole term also contributes only about 0.1 kcal/mol in differential comparisons of dication complexes of a given type. The effective dielectric constant was chosen to be 78 for the hydration models and 4 for the protein models.

Other corrections were made to account for the possible errors due to lack of electronic correlation in the SCF approximation. Interligand dispersion energies, designated disp, are obtained at the simplest correlation level with the Moller–Plesset perturbation method at second order (MP2) using the largest basis and with the basis set superposition error (BSSE) corrected using the counterpoise method. The correlation effect on the metal–ligand interaction was estimated as the MP2 effect computed in the optimization basis on the binding energy of each metal to its complete ligand shell. This definition allows for the basis-set-superposition correction which is essential because the MP2 BSSE is several times larger than the relatively minor BSSE at the SCF level. Pairwise additive estimates of the metal–ligand correlation energies would not be useful because the ligand electron densities are much more heavily polarized when only one ligand is bound to the dication compared to four or more ligands. The estimated correlation effect on the total complex binding energy is designated dBE(MP2) in the Tables II and IV. The MP2 level of correlation has been found to improve binding energies to transition metals compared to experimental values.[27]

The vibrational zero-point-energy (ZPE) gain in forming a complex is obtained as the difference between the complex and monomer ZPE's. The vibrational frequencies were calculated with the 3-21G basis set in the harmonic approximation. Optimized complexes with the 3-21G basis were structurally very similar to those obtained with the larger, polarized CEP basis set. A correction for the loss of hydrogen bonding of first-shell waters is listed as free W in Table IV.

The effect on the electronic structure of the deprotonated tetrahedral CA model of substituting ammonia ligands for imidazole was tested by first replacing one and then all three of the ammonia ligands with imidazole. The imidazole basis was CEP-31G and the rest of the system used the optimization basis described above. Larger basis and MP2 corrections were not feasible for this large system. It was possible to optimize the metal–imidazole distance for the single-substitution models with the other internal coordinates fixed as optimized in the exclusively ammonia model. Imidazole internal coordinates were taken from a microwave structure.[28] The tilt of each imidazole ring relative to the M–N bond was fixed by assuming equal values of its two M–N–C angles (127.55°) with the M–N bond in the ring plane. The single-substitution models were first carried out with the metal–oxygen bond in the ring plane and the dot product of the directed metal–oxygen bond and the imidazole N–C2 bond being positive. After the limited optimization the ring was also rotated by 90° around its M–N axis. The optimized M–N bond distances for imidazole ligands were all within 0.08–0.10 Å shorter than the corresponding values for ammonia given in Table I due to the factor of two increase in ligand dipole moment. The triply-substituted model used these metal–imidazole distances, but the imidazole planes were rotated to have a 45° value for each O–M–N–C2 torsional angle. These structures closely represent a symmetrized version of the known ZnCA first shell.[5]

3. Results and Discussion

Metal substitution in a first-shell model of the CA active site can directly affect the reactive behavior by modifying (a) the coordination number and stereochemistry of the first shell, (b) the electronic structure and nucleophilicity of the MOH moiety, and (c) the effective proton affinity of MOH. The cluster results show that only the coordination number behavior changes substantially with metal substitution and could be related to the lack of activity of CdCA and MnCA. The water-bound complex for ZnCA has been calculated to be five-coordinate with two first-shell waters in an earlier ab initio calculation.[7] However, there is a substantial increase in the binding energy of the second water to a five-coordinate low-pH complex for MnCA and CdCA as indicated in Table III. All the substituted low-pH forms are predicted to be five-coordinate, but as noted above the inclusion of the anionic form of His-119 could alter these conclusions.

With a hydroxide ligand in the high-pH form, the previous ab initio calculations found a preferred second-shell position for a bound water although a local minimum exists for a five-coordinate structure for ZnCA and CoCA.[7,8] However, the increased binding energy of a water in the first shell of CdCA and MnCA compared with ZnCA occurs also for the high-pH complex and suggests that the coordination increases for CdCA and MnCA in both pH forms. Although the binding energy of water in the second shell remains larger for Cd and Mn models, such energetic binding sites should remain available if the first shell expands. Additional evidence supporting the hypothesis of increased coordination of Cd and Mn comes from the study of an inhibitor, thiocyanate anion, which binds to CA with a water molecule in a five-coordinate complex.[29] Our previous study[7] showed that the binding energy of a water molecule in the first shell was very nearly identical whether hydroxyl or thiocyanate anion was already bound, and the observed difference in coordination was thus attributed to environmental influences. Presently, we calculate increased binding energies of 23 and 39 kJ/mol for an additional water molecule at high pH if cadmium and manganese, respectively, are substituted for zinc. The thiocyanate inhibitor displaces the second-shell or "deep" water but does not affect the hydrogen-bonded network connecting the ligands attached to zinc with the His-64 implicated in the proton shuttle. The relatively slight increase in the M–O distance for manganese or even cadmium substitution should also have little effect on the hydrogen-bond network. This suggests that the relatively strongly bound water in the fifth coordination site for cadmium and manganese acts as an inhibitor, altering the rate-limiting step for CdCA and MnCA. The cluster model dramatically simplifies the analysis of the active site of CA but suggests a change in the fundamental coordination behavior as a function of metal substitution.

A four-coordinate structure for CdCA[12] has been deduced from a simple model for the source of the electronic anisotropy that couples to the quadrupole of the Cd nucleus. This model assumes the bonding of Cd to the ligands is by a covalent σ bond when the molecular orbital analysis shows predominant binding by

(24) (a) Probst, M. M.; Radnai, T.; Heinzinger, K.; Bopp, P.; Rode, B. M. *J. Phys. Chem.* **1985**, *89*, 753. (b) Palinkas, G.; Heinzinger, K. *Chem. Phys. Lett.* **1986**, *126*, 251.
(25) Holmes, O. G.; McClure, D. S. *J. Chem. Phys.* **1957**, *26*, 1686.
(26) Wilson, R. B.; Solomon, E. I. *J. Am. Chem. Soc.* **1980**, *102*, 4085.
(27) Kitchen, D. B.; Allen, L. C. *J. Phys. Chem.* **1989**, *93*, 7265.
(28) Christen, D.; Griffiths, J. H.; Sheridan, J. *Z. Naturforsch.* **1982**, *37a*, 1378.
(29) Eriksson, A. E.; Kylsten, P. M.; Jones, T. A.; Liljas, A. *Proteins* **1988**, *4*, 283.

Table V. Mulliken Populations for $MOH(NH_3)_2$(imidazole) Clusters

	Zn	Co	Mn	Cd
		Total Atomic Charge		
M	1.263	1.133 (−2.905)[a]	1.264 (−4.963)	1.364
O	−1.087	−1.035 (−0.045)	−1.063 (−0.053)	−1.108
H(O)	0.440	0.444 (−0.006)	0.442 (−0.002)	0.424
N	−0.943	−0.919 (−0.017)	−0.946 (0.011)	−0.945
		Total Group Charge		
OH	−0.647	−0.590 (−0.051)	−0.621 (−0.055)	−0.684
NH_3	0.128	0.153 (−0.015)	0.119 (0.006)	0.106
		Gross Orbital Populations		
M d	9.970	7.114 (2.877)	5.107 (4.890)	10.000
O s	1.802	1.779 (0.010)	1.784 (0.009)	1.819
O $p_x + p_y$	3.872	3.845 (0.030)	3.829 (0.050)	3.882
O p_z	1.404	1.401 (0.002)	1.439 (−0.008)	1.397
O d	0.008	0.009 (0.002)	0.009 (0.001)	0.009

[a] The excess α spin population is given in parentheses.

Table VI. Mulliken Populations for $MOH(NH_3)_2$(imidazole) Clusters

	Zn	Co	Mn	Cd
		Total Group Charge		
M	1.287	1.191 (−2.929)[a]	1.311 (−4.960)	1.387
OH	−0.656	−0.609 (−0.046)	−0.631 (−0.057)	−0.694
NH_3	0.118	0.137 (−0.010)	0.108 (0.006)	0.098
imidazole	0.132	0.145 (−0.005)	0.104 (0.005)	0.110
		Gross Orbital Populations		
M d	9.980	7.172 (2.913)	5.190 (4.866)	10.014
O s	1.803	1.792 (0.003)	1.785 (0.009)	1.820
O $p_x + p_y$	3.878	3.830 (0.057)	3.838 (0.048)	3.888
O p_z	1.398	1.409 (−0.004)	1.434 (−0.006)	1.394
imid σ	19.866	19.859 (0.001)	19.898 (−0.007)	19.890
imid π	6.002	5.996 (0.004)	5.998 (0.002)	6.000

[a] Excess α spin population is given in parentheses.

electrostatics and polarization of the ligands. Charge transfer from the ligand to the Cd dication will provide a polarized population of much less than one electron in the Cd 5p orbital that can couple to the nucleus. This 5p population, however, will increase as the pH is increased and the ligated water ionized to hydroxyl anion. This would qualitatively explain the large increase in the average coupling in the high-pH form. Relating the anisotropy of the coupling to the structure will not be attempted here, but the experimental structure of the low- and high-pH forms of CdCA have not been definitely deduced as yet.

Only small changes in nucleophilicity are predicted by the Mulliken partial charges on oxygen for the various metal-substituted models. We are assuming that comparable charge distributions for different metal-substituted model compounds implies a comparable nucleophilicity. The change in populations with metal substitution is compared in Table V for ammonia complexes with linear MOH and other internal coordinates at optimum values. The range of charge found for the OH moiety in zinc and cobalt models allows for a low activation energy attack of OH on carbon in CO_2. Both CdCA and MnCA have a total group charge for OH that is larger than that for CoCA. As expected the larger Cd ion attracts less charge, resulting in an even more negative oxygen than for zinc. Very similar patterns are observed in Tables VI and VII with imidazole tripods with even less overall charge transferred from oxygen.

In the manganese complexes there is an apparent shift in the relative binding strength of oxygen and nitrogen lone pair electrons, with the oxygen bonds relatively stronger than for the other metals. This was observed for both pH models by pulling either the tripod or the oxygen ligand out to infinity without reoptimization. The effect is more noticeable for the high-pH model and is indicated in Figure 4a as a dip in the tripod binding to $MnOH^+$ and a rise in the hydroxyl binding to $(NH_3)_3Mn^{2+}$ when plotted versus the hydration radii. This could indicate an enhanced metal–ligand π-bonding interaction with Mn, also leading to the larger MnOH optimum angle for bound hydroxyl.

Table VII. Mulliken Populations for $MOH(imidazole)_3$ Clusters

	Zn	Co	Mn	Cd
		Total Group Charge		
M	1.307	1.208 (−2.924)[a]	1.344 (−4.953)	1.409
OH	−0.658	−0.606 (−0.052)	−0.636 (−0.057)	−0.696
imidazole	0.117	0.133 (−0.008)	0.097 (0.003)	0.096

[a] Excess α spin population is given in parentheses.

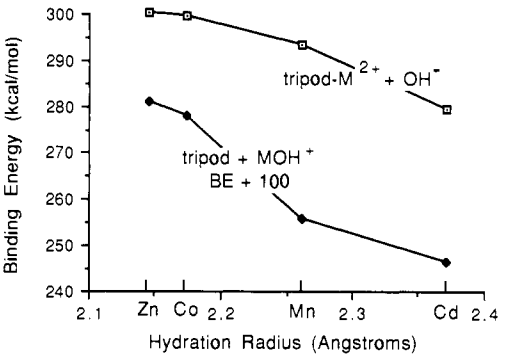

Figure 4. Binding energy of both OH^- and MOH^+ as (a) a function of the metal-to-oxygen binding distance or hydration radius and (b) a function of the radius of $M^{2+}(NH_3)_3$ complexes.

It is apparent that CoCA and MnCA receive excess charge transfer from their ligands since they do not follow the trend observed with ZnCA and CdCA where an increase in size reduces the ligand to metal charge transfer. For ZnCA and CdCA, charge can only transfer into the open sp valence shell while for Co and Mn there are also unoccupied d orbitals. The additional charge is traced to spin-polarized charge transfer in the amount of 0.095 electron for Co and 0.037 electron for Mn, but most of the electron transfer is to the unoccupied sp orbitals of the Co and Mn dication as in the case of zinc and cadmium. In the case of Mn, the spin-polarized charge transfer is dominated by transfer from the oxygen π orbitals, with the metal-bonded σ orbitals for both the oxygen and nitrogen atoms contributing little. With the z axis oriented along MOH, the d_{xz} and d_{yz} orbitals of Mn are properly positioned to accept charge transfer from the oxygen π orbitals. We suggest that the stabilization energy due to charge transfer from oxygen ligands is the cause of the relatively favorable binding seen in Figure 4a. This additional charge transfer could weaken the binding to the tripod, but the similar patterns of binding the tripod to MOH^- and M^{2+} shown in Figure 4a suggest that this is not a major effect. The same binding energies are also plotted in Figure 4b against radii obtained from optimizing $M(NH_3)_3$ complexes. Electrostatic arguments would predict a nearly linear plot of binding energies versus radii but with a slight concave curvature with magnitude dependent on the charges and dipoles of the interacting groups. The Mn^{2+} and $MnOH^-$ species behave as expected for binding to the tripod, but $Mn^{2+}(NH_3)_3$ shows a substantial excess for OH^-.

Analogous charge transfer is observed from oxygen π orbitals into dπ orbitals on Co. Very little transfer is observed from the metal-bonded σ orbital into the essentially open d_{z^2} orbital presumably because this orbital is substantially more antibonding with respect to the hydroxyl anion. The π orbital transfer is not energetically favorable in this case because the dπ orbitals on Co are already partially occupied. The charge transfer does have the effect of increasing the d shell radii by 7% for Mn and 6% for Co over the free ion values, while the zinc and cadmium closed shell d radii increase by only 1 or 2% in the complex. The relative importance of π orbital charge transfer raises the concern of modeling the histidines in CA with nitrogen ligands that do not have π orbitals oriented to transfer or accept charge.

The data in Tables VI and VII, however, show that the π ring systems in a complete first shell do not contribute significantly to the charge transfer. Charge transfer per ligand in these dicationic complexes is lowered as ligands are added to complete the shell due to the combined repulsive effect of the ligands toward

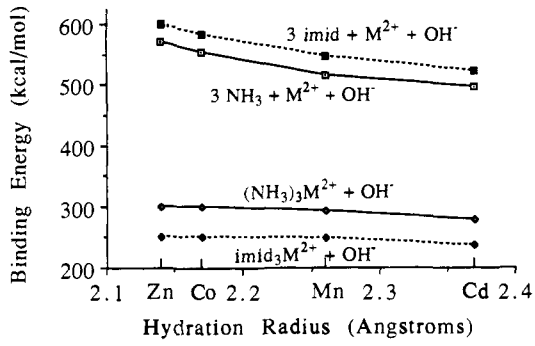

Figure 5. Comparison of total and hydroxyl binding energies for the ammonia and imidazole tripods.

the additional charge density around the dication. The total and hydroxyl binding energies are compared for the different tripods in Figure 5. The pattern is similar with respect to metal substitution although the overall gradient in properties in going from Zn to Cd is reduced by approximately 25%. The substitution of ammonia by imidazole illustrates the behavior of the charge transfer in a complete first shell of ligands. The first imidazole that is substituted transfers more charge than the ammonia, but inhibition of the transfer from the remaining ammonias by the larger imidazole dipole moment dominates. After the complete substitution in the tripod, the imidazoles inhibit each other so that each transfers less than in the singly-substituted model. Reduced charge transfer also reduces the binding energy of the hydroxyl as seen in Table V. This would also increase the M–O distances over the ammonia tripod results if the geometry optimizations were performed. The larger total complex binding energies are due to the larger imidazole dipole moment.

The metal binding energies to CA in Tables II and III are calculated relative to the calculated hydration enthalpies. The calculation errors in the total binding energies are assumed to cancel between the CA and hydration models. The calculated data for the four-coordinate complexes predict the same ordering of the stability for the low- and high-pH models and therefore correctly predict a pH independence for the relative stability.[3,14,30] The relative stabilities for HCAB enzyme at low pH converted to binding enthalpies are 0, 7.5, 18.8, and 38.5 kJ/mol, respectively. The experimental stability ordering of Zn > Cd > Co > Mn is reproduced by the tetrahedral models over the entire pH range with the predicted spread in binding constants being roughly 50% too wide. Second-shell addition of a water does not change the order of binding. Addition of water to the first shell reduces the spread of binding constants by increasing the stability of the MnCA and CdCA models relative to ZnCA. The incorrect prediction of greater stability of CdCA over ZnCA for the five-coordinate low-pH model is an indication of the errors inherent in the simple model. The most that could be expected from a first-shell model is the qualitative agreement with experiment that finds the stable clusters relate to the stable metalloenzymes while the less stable clusters represent the weakly bound CoCA and MnCA. The much weaker binding of manganese to CA observed experimentally and predicted by the cluster model is explained by the charge-transfer effects from the oxygen ligand to d orbitals of the Mn cation.

Comparing the calculated hydration enthalpies to experimental values in Table IV shows that the qualitative behavior is obtained with the simple first-shell model. Both the Jahn–Teller and large correlation correction significantly improve the agreement for cobalt. All of the calculated M–O distances of the hexaaquo ions agree with experiment to within 0.07 Å.[23] The relative enthalpies compare well with experiment except for cadmium. The similarity in the radial dimensions of the calculated cadmium and calcium first shells raises a caveat regarding the 6-fold coordination. Recently, neutron data for calcium have been interpreted in terms of a nine or even ten coordination,[24] suggesting that the first shell in cadmium may also be larger than six coordinate. We first investigated the nine-coordinate complex but found the calculated distance, R(Cd–O), increased by about 0.3 Å. For this reason, an eight-coordinate structure was optimized, increasing the first-shell radius by only 0.11 Å and obtaining a hydration enthalpy slightly larger than that for the six-coordinate complex. However, the calculated enthalpy still has a considerable discrepancy relative to experiment, leaving the question of the first-shell coordination number of hydrated Cd^{2+} unresolved.

Radial optimization of the zinc and cobalt complexes at the MP2 level has a substantial effect on the comparison of the hydration energy because of the larger correlation component of the ligand binding for cobalt. The optimization decreased the zinc–oxygen distances to 2.11 Å and the cobalt–oxygen average distance to 2.12 Å, resulting in a gain in stability of 3.3 kJ/mol for the cobalt complex relative to the zinc. The relatively smaller size of hexaaquo cobalt yields a larger increase of 8.4 kJ/mol in the relative stability of cobalt hydration by recalculating the Born energy of the MP2 cobalt and zinc structures. After these corrections, the cobalt hydration energy is predicted to be 3.8 kJ/mol larger than that for zinc, which is in better agreement with the experimental results than the entries in Table IV based on the UHF optimized geometries. The magnitude of the correlation correction for manganese and cadmium complexes is more similar to that for zinc, and therefore, MP2 radial optimization is not expected to affect the qualitative comparisons between these dications.

The comparison between the EPA for a high-pH four-coordinate ZnCA and five-coordinate CdCA and MnCA cannot be done with any accuracy with a simple Born model. The five-coordinate high-pH models yield an acceptable range and separation of the EPA. If it is assumed that for all substituted CA the high-pH form is four-coordinate and the low-pH form five-coordinate, it is seen that the order of the relative EPA and experimental pK_a is maintained but the magnitude of the differences between the EPA is larger than found experimentally. The range of effective proton affinities (EPA) for the tetrahedral complexes is found from Table II to be 23.0 kJ/mol. This corresponds to a pK_a spread of about 4 units while the experimentally observed spread is about 3 units,[3] but the order of the calculated and observed pK_a are in agreement. The manganese and cadmium dications are predicted to produce larger complexes (see Table I) and, therefore, reduce the proton affinity of hydroxyl anion by a lesser amount than zinc due to a weaker electrostatic influence of the dication at the protonation site. The largest dication, cadmium, leads to the largest EPA, as found experimentally, but the predicted pK_a difference from the MnCA is 2 units while a 1-unit difference is observed experimentally. The CoCA complex is slightly larger than the ZnCA, but nevertheless it has a lower effective proton affinity by about 1 unit, agreeing with the observed behavior. This results in the present calculation primarily from a small shift in the differential binding due to electron correlation.

The correlation energy contribution to ligand binding with cobalt (Table II) is anomalously large for these cations, reflecting the higher density of low-lying metal states whose excitation contributes to the correlation energy of this transition metal dication. It is also comparable for both the low- and high-pH forms. We have investigated whether correlation might also lead to geometric changes sufficient to yield significant differential energetics by optimizing the radical distances for the tetrahedral complexes of ZnCA and CoCA at the MP2 level. The high- and low-pH zinc complexes both have metal–ligand distances decrease by only 0.02 Å while the proton affinity is unchanged. The cobalt complexes shrink by 0.04 Å, bringing their sizes into close agreement with the zinc, but the EPA decreases by only 0.4 kJ/mol. Changes in the Born energies due to these geometric contractions increase the CoCA EPA by 2.2 kJ/mol relative to ZnCA. It is apparent that optimization at the MP2 level would not change the results significantly.

The relation between the ordering of the EPA and the pK_a of the substituted enzymes for this model is significant for the insight into the electronic structure of the first-shell active site. The

(30) Lindskog, S.; Nyman, P. O. *Biochim. Biophys. Acta* **1964**, *85*, 462.

absolute values and the spread of the effective proton affinities (EPA) are model dependent since the protein and solvent polarization are not considered in detail and the model is both static and highly simplified. Local bonding networks of hydrogen bonds to both the histidine tripod and the water and hydroxide ligands would profoundly affect the magnitude of the EPA. For example, we have recently shown that the ionicity of the first-shell complex is a function of the pH, and proton transfer between the first and second shell of the active site modulates the EPA.[7] The effect of the active site fields and, in particular, the presence of partially ionic H bonds to the active site Thr-199 has also been shown to be large.[31] The basic assumption in the persent calculation is the dominance of the metal-binding interaction in the first shell of the active site in determining the EPA, and the relative EPA are obtained if the metal substitution does not alter the first shell too much.

Examination of Table II shows the number of different factors that are important in determining the EPA. The Born estimate of the reaction field interaction is the most significant. The cavity radius increases by about 0.25 Å in going from ZnCA to CdCA. This leads to a relative stabilization of ZnCA in the protonated state while the high-pH complex has roughly constant Born energy for all the dications. Consequently, the spread in the EPA is reduced by about 7 kcal/mol relative to the SCF cluster values. In one case, the higher moment contributions to the Born energy have a qualitative effect on the relative EPA values. The reaction field stabilization energy of the MnCA high-pH model is smaller than that for the larger CdCA cluster. This is because of the larger M-O-H angle found for Mn (see Table I), giving a more symmetric cluster with smaller dipole and quadrupole moments leading to a smaller reaction field energy.

(31) Cook C. M.; Haydock, K.; Lee, R. H.; Allen, L. C. *J. Phys. Chem.* **1984**, *88*, 4875.

MNDO Study of Boron-Nitrogen Analogues of Buckminsterfullerene

Xinfu Xia,[†] Daniel A. Jelski,*[,‡] James R. Bowser,[‡] and Thomas F. George[§]

Contribution from the Department of Chemistry, State University of New York at Buffalo, Buffalo, New York 14260, Department of Chemistry, State University of New York, College at Fredonia, Fredonia, New York 14063, and Departments of Chemistry and Physics, Washington State University, Pullman, Washington 99164. *Received January 27, 1992*

Abstract: An MNDO study of boron-nitrogen analogues of buckminsterfullerene is presented. The relative properties of ($@C_{60}$), ($@B_2C_{58}$), ($@N_2C_{58}$), ($@BNC_{58}$), ($@C_{12}B_{24}N_{24}$), and ($@B_{30}N_{30}$) are studied. The heats of formation of such 60-atom systems from benzene, naphthalene, and their BN analogues are compared. It is found that all these hybrids are approximately as stable as buckminsterfullerene. Surprisingly, it is predicted that ($@B_{30}N_{30}$) will be stable and should be relatively simple to synthesize from borazine.

I. Introduction

Recent experiments have shown that individual boron atoms can displace carbon atoms in the bucky ball molecule, creating "dopey ball" fullerene structures with the stoichiometry ($@B_nC_{60-n}$), where n ranges from 1 to 6.[1] The @ symbol indicates a closed fullerene structure with all atoms forming an integral part of the cage framework.[2] While it has not yet been demonstrated, it seems reasonable that BN analogues of buckminsterfullerene could also be synthesized. It has been suggested[1] that ($@B_{30}N_{30}$) would not be stable since it would require that N-N and B-B bonds exist in the molecule, presumably destabilizing it. In particular, it is supposed that N-N σ-bonds would be unfavorable.

In response to this suggestion, we have proposed a molecule in which the largest possible number of carbons are substituted subject to the constraint that there be no B-B or N-N bonds.[3] This turns out to imply that each pentagon must contain one carbon atom, yielding the stoichiometry ($@C_{12}B_{24}N_{24}$); the optimal structure is shown in Figure 1 and belongs to the S_6 point group. A simple Hückel calculation indicated that it would be more stable than buckminsterfullerene. Nothing in what follows changes that conclusion, although we now have considerably more information to report.

We describe here the results of an MNDO study of boron-nitrogen analogues of buckminsterfullerene. Given computational limitations, we are essentially limited to closed shell systems and hence are restricted to an even number of substituted atoms. Thus we consider ($@C_{60}$), ($@B_2C_{58}$), ($@N_2C_{58}$), ($@BNC_{58}$), ($@C_{12}B_{24}N_{24}$), and ($@B_{30}N_{30}$). There are obviously many possible isomers of most of these species, and we consider several of each.

Table I. Calculated vs Experimental Enthalpies of Formation for Selected Compounds

compound	$\Delta H_f°$ (kcal/mol) MNDO	exptl	ref
C_6H_6	+21.3	+19.8	4
$C_{10}H_8$	+38.3	+36.1	4
$B_3N_3H_6$	-131.1	-124	5
$C_2B_4N_4H_8$	-132		
$B_5N_5H_8$	-225.5		
C_{60}	+869.3	+545	10

In order to establish the accuracy of our method, we have compared the MNDO calculated heats of formation for benzene, naphthalene, and borazine with experimental values. It is seen that the MNDO calculation overestimates all of these formation enthalpies by about 7%. The data are given in Table I, along with those for two naphthalene analogues. While we have found no comparable experimental data for the latter, this information will be useful in what follows.

[†] SUNY at Buffalo.
[‡] SUNY, College at Fredonia.
[§] Washington State University.

(1) Guo, T.; Jin, C.; Smalley, R. E. *J. Phys. Chem.* **1991**, *95*, 4948.
(2) Chan, Y.; Guo, T.; Jin, C.; Haufler, R. E.; Chibante, L. P. F.; Fure, J.; Wang, L.; Alford, J. M.; Smalley, R. E. *J. Phys. Chem.* **1991**, *95*, 7564.
(3) Bowser, J. R.; Jelski, D. A.; George, T. F. *Inorg. Chem.* **1992**, *31*, 154.

0002-7863/92/1514-6493$03.00/0